

Laboratory Insight into the Evolution of the Seismic Potential of an Asperity due to Wear

Sofia Michail¹, P.A. Selvadurai¹, M. Rast², A.F. Salazar Vásquez^{1,3}, P. Bianchi¹, C. Madonna², S. Wiemer¹

¹Swiss Seismological Service, ETH Zurich; ²Geological Institute, Department of Earth Sciences, ETH Zurich;

³School of Architecture, Civil Engineering, Landscape Architecture Spatial Planning, Eastern Switzerland University of Applied Sciences



Introduction and Motivation

Faults in nature exhibit complex surface characteristics, such as the presence of contact asperities, which affect the potential for earthquake nucleation. A common metric to study frictional stability is the nucleation size h^* , which can change due to spatial heterogeneity⁽¹⁾ and wear. Here we use novel laboratory methods to investigate parameters controlling h^* ^(2,3) and how they likely changed during our experiment. Wear created surface conditions that eliminated off-fault strain accommodation and nullified the asperities seismogenic potential of the fault.

$$h^* \sim \frac{GD_c}{(b-a)\sigma_n}$$

- G : Shear modulus
- D_c : Critical Slip distance
- $(b-a)$: Rate and state friction parameter⁽³⁾
- σ_n : Normal stress

Methodology

We performed a triaxial experiment at sequentially increasing confining pressures ($P_c = 60, 80, 100$ MPa) on a saw-cut sample of Carrara marble.

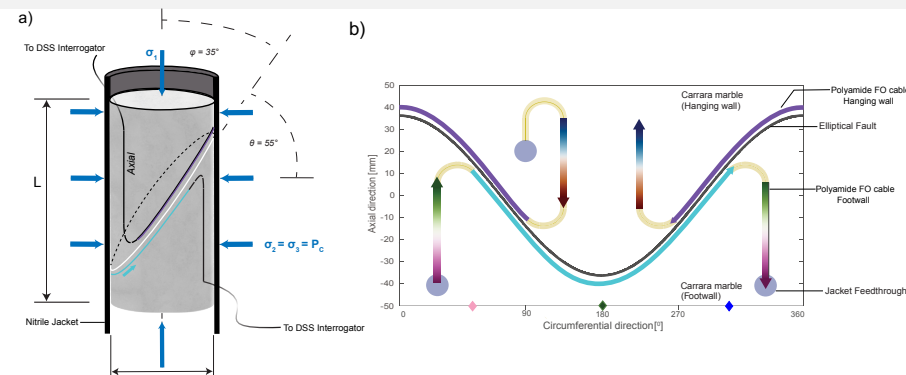


Figure 1. (a) Schematic representation of the saw-cut sample of Carrara marble under triaxial loading. The location of the FO cables attached to the sample's surface is shown as black and purple curves on the hanging wall and as cyan and black curves on the footwall. (b) The distributed strain sensing (DSS) layout is shown on an unwrapped perspective.

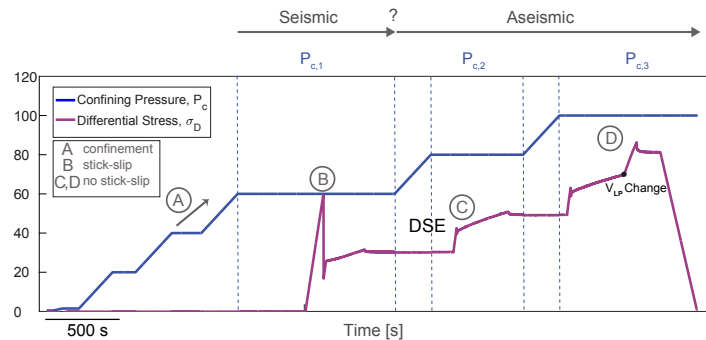


Figure 2. Temporal evolution of the confining pressure P_c and differential stress $\sigma_1 - \sigma_3$ during the experiment. The three frictional tests are depicted with $P_{c,1}$, $P_{c,2}$, and $P_{c,3}$ and the stick slip event DSE.

Mechanical Data and Numerical Model

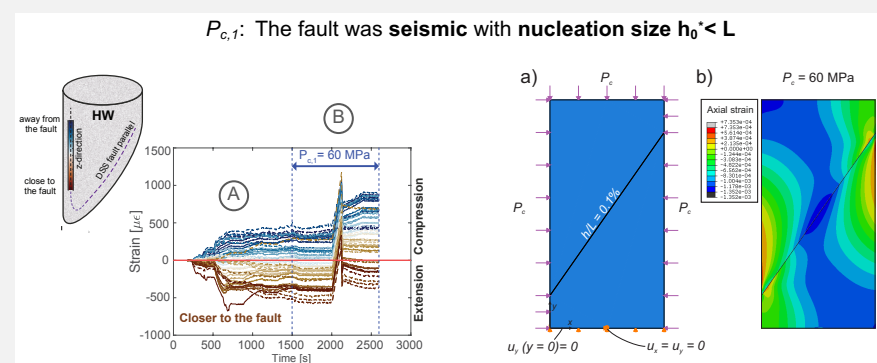


Figure 3. Spatio-temporal evolution of the DSS axial strain of the hanging wall (HW).

Figure 4. (a) FEM model used to simulate contact stresses in a triaxial with curved interface geometries. (b) Axial stress (LE22 in ABAQUS) through the sample for confining pressure $P_{c,1} = 60$ MPa.

Figure 5. Height measurements with stylus profilometry of the HW fault interface (pre and post experimental).

Figure 6. Image of the post-mortem fault surface of the HW.

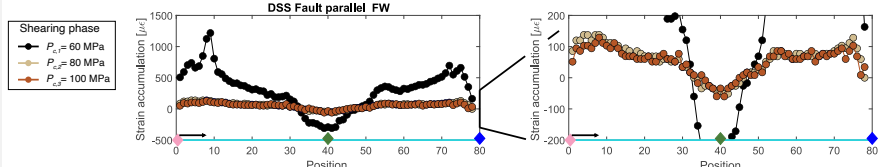


Figure 6. Spatio-temporal evolution of fault parallel strain (DSS fp strain) of FW during the three shearing phases of the peak friction experiment.

Surface Characterization

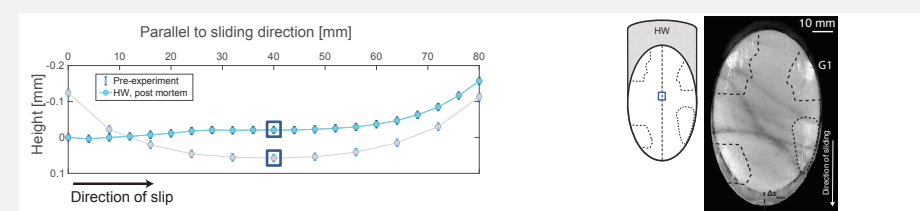


Figure 5. Height measurements with stylus profilometry of the HW fault interface (pre and post experimental).

Figure 6. Image of the post-mortem fault surface of the HW.

Figure 7. Optical Profilometry images of two sections in the center of the central asperity of the HW (a) pre-experimental (b) post-experimental and (G) a gouge location.

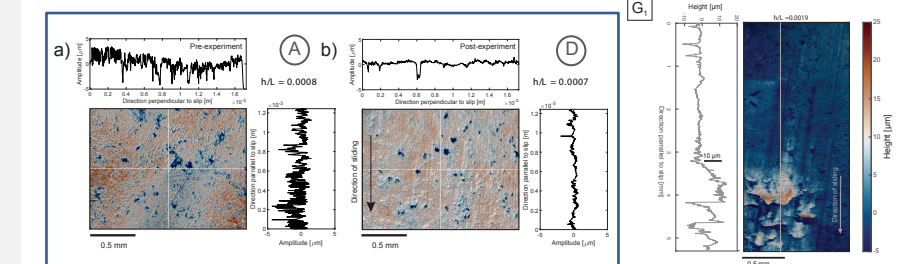


Figure 7. Optical Profilometry images of two sections in the center of the central asperity of the HW (a) pre-experimental (b) post-experimental and (G) a gouge location.

The central asperity smoothed due to wear after the DSE. Gouge has been deposited closer to the fault periphery. The gouge accommodates strain in the shear bands, resulting in low DSS fault parallel strain.



Figure 8. Schematics of the effect of gouge on the strain and slip during the subsequent steps of the experiment.

Figure 9. Transmitted light micrograph of a gouge shear band (by Verberne et al., 2014).

Conclusions

- Axial DSS measurements showed extensional strain during confinement. Stylus profilometry revealed a central asperity with $h/L = 0.1\%$. This strain heterogeneity due to the asperity was further confirmed by our FEM model. **This asperity dominated the contact conditions and led to dynamic nucleation (DSE).**
- After the DSE, the central asperity was worn and gouge was deposited. The DSS fp strain decreased. **The new contact conditions were dominated by the gouge and no dynamic nucleation was observed. The vs gouge⁽⁴⁾ resulted to (a-b) changes and therefore aseismic conditions.**

References

- Selvadurai, P.A., Galvez, P., Mai, P.M., Glaser, S.D., 2023. Modelling frictional precursory phenomena using a wear-based rate- and state dependent friction model in the laboratory. *Tectonophysics* 847. doi:10.1016/j.tecto.2022.1011.229689
- Aubry, J., Passelegue, F.X., Escartin, J., Gasc, J., Deldicque, D., Schubnel, A., 2020. Fault Stability Across the Seismogenic Zone. *Journal of Geophysical Research: Solid Earth* 125. doi:10.1029/2020JB019670
- Rubin A. and Ampuero J. 2008. Earthquake nucleation on (aging) rate and state faults, *Journal of Geophysical Research: Solid Earth* 110. doi: 10.1029/2005JB003686
- Verberne, B.A., Spiers, C.J., Niemeijer, A.R., De Bresser, J.H., De Winter, D.A., Plümpner, O., 2014. Frictional Properties and Microstructure of Calcite-Rich Fault Gouges Sheared at Sub-Seismic Sliding Velocities. *Pure and Applied Geophysics* 171, 2617–2640 doi:10.1007/s00024-013-0760-0